

The stability of nonequilibrium molecular dynamics simulations of elongational flows

B. D. Todd^{a)}

Computer Simulation and Physical Applications Group, School of Information Technology, Swinburne University of Technology, P.O. Box 218, Hawthorn, Victoria 3122, Australia

Peter J. Daivis^{b)}

Department of Applied Physics, RMIT University, GPO Box 2476V, Melbourne, Victoria 3001, Australia

(Received 7 September 1999; accepted 1 October 1999)

We show that nonequilibrium molecular dynamics simulations of elongational flows are inherently unstable over long periods of time. This instability leads to a catastrophic nonequilibrium phase transition that destroy the true structure of the fluid. We identify the source of this instability as a lack of momentum conservation, resulting from numerical round-off errors. We show that this error grows exponentially in the direction of compression, and present two numerical recipes that involve only minor perturbations to the particle trajectories to guarantee momentum conservation. © 2000 American Institute of Physics. [S0021-9606(99)51748-0]

INTRODUCTION

The study of steady, time-independent elongational flow of atomic fluids by nonequilibrium molecular dynamics (NEMD) techniques has until recently been restricted to very short total simulation times. The reason for this is in the nature of the flow geometry, where to guarantee volume conservation the fluid must contract in at least one dimension as it simultaneously expands in at least one other. Thus, the simulation comes to a halt when the length of the simulation cell in the contracting dimension reaches its minimum extension of twice the potential interaction cutoff radius.

Only recently has this limitation been overcome by application of the spatially and temporally periodic boundary conditions devised by Kraynik and Reinelt.¹ While applicable only to planar elongational flow (i.e., contraction in one direction, expansion in another, while the third remains unchanged), the method has nonetheless allowed the first long-time simulations of steady, time-independent elongational flow by NEMD simulations.^{2–4} These first papers were mainly concerned with demonstrating that the method of Kraynik and Reinelt¹ could successfully be applied to NEMD simulations, and on developing algorithms that are highly efficient and analogous to standard NEMD simulations of planar Couette flow.⁴ As such, they did not attempt to simulate planar elongational flow for more than a few thousand time steps, as this was sufficient to demonstrate the soundness of the algorithms.

In this paper we simulate planar elongational flow over hundreds of thousands of time steps. We will show that for relatively weak elongation strain rates the simulation is unstable and induces a catastrophic nonequilibrium phase transition in the fluid. We further show that such a phase transition is a consequence of the nonconservation of a total peculiar momentum resulting from an exponential growth of

numerical round-off error. This exponential growth of round-off error has not previously been discussed, but is in fact common to *all* NEMD simulations, where compression in at least one dimension occurs. It would never have been observed before because of the long simulation times required for the effects to manifest themselves clearly. We demonstrate that this kind of numerical error does not occur in standard NEMD simulations of planar Couette flow, but is unavoidable when simulating elongation and is independent of the type of numerical integrator chosen. Finally, we propose two simple numerical recipes involving only minor perturbations to the particle trajectories that overcome this problem and guarantee the conservation of total peculiar momentum for arbitrarily long total simulation times.

SIMULATIONS AND RESULTS

As stated in the Introduction, our purpose in this paper is to demonstrate that all previously existing NEMD algorithms of planar elongational flow are inherently unstable. The instability induces a catastrophic phase transition in the fluid, which is nothing more than an artifact of the simulation algorithm. In this paper we use the “deforming-brick” algorithm we previously devised to simulate planar elongational flow (PEF).⁴ To ensure that the effects we observed were independent of the type of algorithm used, we also performed some test simulations using the “Lagrangian-rhomboid” algorithm,⁴ our original simulation algorithm (in which the simulation cell is always skewed with respect to the flow axes),² and the now redundant method of simulating the flow with the axes of the simulation cell aligned with the flow fields.^{5–8} We observed exactly the same numerical errors in all these algorithms. The test of the latter algorithm was to ensure that the problem was not a consequence of the Kraynik–Reinelt method, which is extremely important if this method is to be a viable “standard” procedure for performing NEMD simulations of PEF. Furthermore, we tested the algorithms using both fifth-order Gear predictor–

^{a)}Electronic mail: btodd@swin.edu.au

^{b)}Electronic mail: peter.daivis@rmit.edu.au

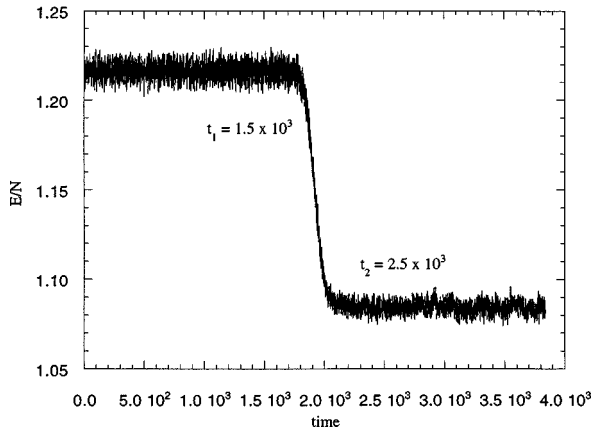


FIG. 1. Total internal energy per particle as a function of time, for a two-dimensional system of 200 WCA particles under planar elongational flow. The system is thermostatted to a temperature of $T=0.722$, and the elongation rate is $\dot{\epsilon}=0.05$. The number density is $N/V=0.8442$. At $t=t_1$ the system undergoes a catastrophic nonequilibrium phase transition. The energy decreases rapidly between $t_1 < t < t_2$, until it reaches a final steady state at $t > t_2$, where it is minimized.

corrector and fourth-order Runge–Kutta numerical integrators, and found that the numerical instability was independent of which type of integrator we used. We also performed simulations on two- and three-dimensional fluids, once again finding that the same problem arose, independent of the dimensionality of the fluid. To ensure that numerical errors were not induced by too large a time step, we performed simulations in which the time step ranged between 10^{-5} – 4×10^{-3} reduced time units and found the numerical instability to be independent of the time step used. For the purposes of demonstration, we will only report the results for a two-dimensional WCA fluid⁹ undergoing PEF, in which the equations of motion are integrated by a fifth-order Gear predictor–corrector scheme. The time step used for the simulations reported in this paper was 0.004 reduced time units. In all simulations, the total number of WCA atoms was 200, while the reduced temperature and number density were 0.722 and 0.8442, respectively. Once again, the effects of changing the temperature, density, size of the simulation cell, and total number of atoms were tested, but none of these tests had any effect on the numerical stability of the flow. Finally, we note that the details of the deforming-brick algorithm, as well as the appropriate SLLOD equations of motion, may be found in Ref. 4, and will not be detailed in this paper.

In Fig. 1 we display the total internal energy per particle for a two-dimensional fluid under PEF, with an elongation rate of $\dot{\epsilon}=0.05$. Our geometry is such that the strain rate tensor is given as

$$\nabla \mathbf{u} = \begin{pmatrix} \dot{\epsilon} & 0 \\ 0 & -\dot{\epsilon} \end{pmatrix}.$$

At times less than $t_1 \approx 1.5 \times 10^3$ reduced time units (corresponding to 375 000 time steps) E/N appears to be constant, as expected. However, between t_1 and $t_2 \approx 2.5 \times 10^3$ E/N

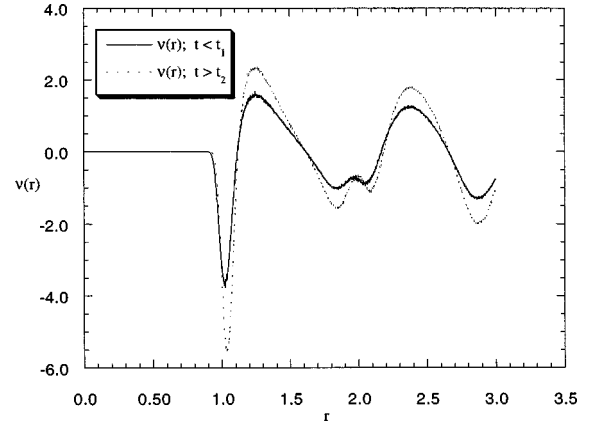


FIG. 2. Radial part of the nonequilibrium component of the total pair distribution function, $v(r)$, for times $t < t_1$ and $t > t_2$. Clearly the fluid structure is altered significantly between $t_1 < t < t_2$.

decreases rapidly. At times greater than t_2 the energy stabilizes again, but at a significantly lower value than its initial “steady-state” value of $E/N \approx 1.215$.

This catastrophic transition in the fluid energy is a result of a flow-induced change in the structure of the fluid. Such nonequilibrium phase transitions have been observed previously in simulations^{10,11} and have been shown to be artifacts of an inappropriate use of profile-biased thermostats.^{11,12} To demonstrate that the fluid has indeed changed its structure, we plot only the *radial* part of the nonequilibrium component of the total pair distribution function, $v(r)$, for (a) $t < t_1$, and (b) $t > t_2$ in Fig. 2. In calculating $v(r)$ we first expand the *total* pair distribution function as a Taylor series, and consider only terms that are first order in the gradient of the streaming velocity,¹³ i.e.,

$$G(\mathbf{r}, \nabla \mathbf{u}) = g(r) + v(r) \left(\frac{\mathbf{r}\mathbf{r}}{r^2} \right) : \nabla \mathbf{u}(\mathbf{r}) + \left(v_0(r) - \frac{1}{3} v(r) \right) \nabla \cdot \mathbf{u}(\mathbf{r}), \quad (1)$$

where $g(r)$ is the equilibrium pair distribution function. For constant volume deformation $\nabla \cdot \mathbf{u}(\mathbf{r}) = 0$, and so Eq. (1) simplifies to

$$G(\mathbf{r}, \nabla \mathbf{u}) = g(r) + v(r) \left(\frac{\mathbf{r}\mathbf{r}}{r^2} \right) : \nabla \mathbf{u}(\mathbf{r}). \quad (2)$$

Following the procedure outlined by Pryde^{14–16} in calculating $v(r)$ for shear flow, one can show that $v(r)$ for a two-dimensional fluid elongating in the x direction and compressing in the y direction is given as

$$v(r) = \frac{1}{\dot{\epsilon}} \left[\frac{\langle x_{ij}^2 \rangle}{\langle r_{ij}^2 \rangle} - \frac{\langle y_{ij}^2 \rangle}{\langle r_{ij}^2 \rangle} \right], \quad (3)$$

where ρ is the fluid density, $x_{ij} = x_i - x_j$, $y_{ij} = y_i - y_j$, $r_{ij} = r_i - r_j$, and the averaging is performed in a small region of the fluid between r and $r + dr$.

It is clear from Fig. 2 that the fluid structure is significantly altered after the phase transition occurs.

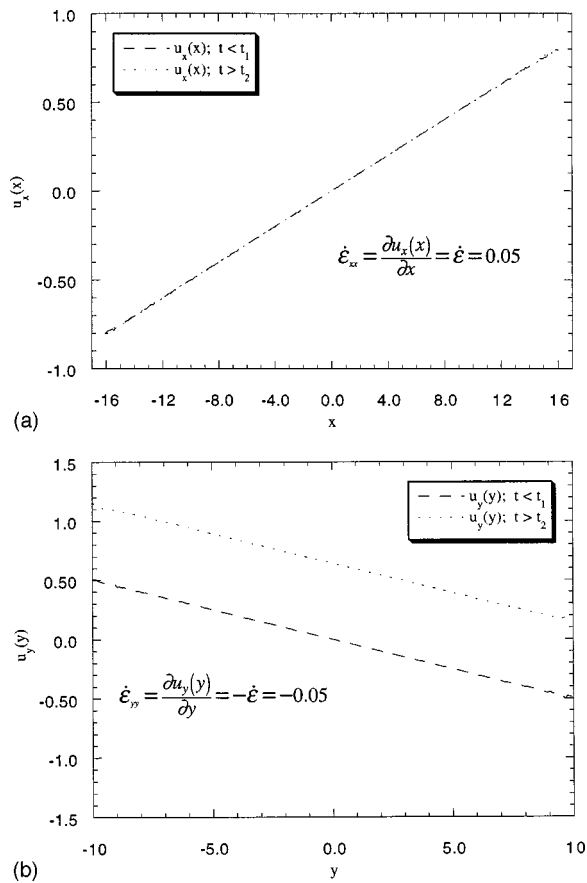


FIG. 3. (a) x component of the streaming velocity for times $t < t_1$ and $t > t_2$. (b) y component of the streaming velocity for times $t < t_1$ and $t > t_2$. At $t > t_2$ $u_y(y)$ is shifted by $\approx +0.51$, destroying the symmetry of the flow in the contracting direction and contradicting the assumptions of the SLLD equations of motion. Note, however, that $\partial u_y(y)/\partial y = -\dot{\epsilon}$, as required by (and input into) the equations of motion.

Of further interest is to look at the actual values of the streaming velocity components in both the x and y directions before and after the transition. If the phase transition is a consequence of an incorrect assumption about the value of the streaming velocity of the fluid, then we may well expect string phases to occur. We calculate the streaming velocity as a function of position by the expression

$$\mathbf{u}(\mathbf{r}, t) = \frac{\rho \mathbf{u}(\mathbf{r}, t)}{\rho(\mathbf{r}, t)} = \frac{\sum_i m \mathbf{v}_i(t) \delta(\mathbf{r} - \mathbf{r}_i(t))}{\sum_i m \delta(\mathbf{r} - \mathbf{r}_i(t))}, \quad (4)$$

where $\rho \mathbf{u}(\mathbf{r}, t)$ is the momentum current density, $\rho(\mathbf{r}, t)$ is the mass density, and $\mathbf{v}_i(t)$ is the laboratory velocity of atom i . In practice, we integrate (or average) $\rho \mathbf{u}$ over a small region, \mathbf{r} . In this example, we divide the fluid into bins of constant thickness Δ_x and Δ_y in the x and y dimensions, respectively. These bins are dynamic, in that the number of bins in the contracting y direction decreases as a function of time (as the cell length in this direction decreases), while the number of bins in the expanding x direction increases. Thus, the statistics for bins will be best nearer the center of the simulation cell, and poorest toward the edges. However, by averaging over many independent simulations we significantly improve the overall statistics.

In Fig. 3 we display the x and y components of the

streaming velocity for times $t < t_1$ and $t > t_2$, as before. The streaming velocity in the expanding x direction, $u_x(x)$ is both linear and identical for both time regions. The elongation rate, given as $\dot{\epsilon}_{xx} = \partial u_x(x)/\partial x = \dot{\epsilon}$ is 0.05, as expected. Of significant interest, however, is $u_y(y)$. Clearly now $u_y(y)$ is *not* the same for both time regions, even though, as required, the slope is correctly determined as $\dot{\epsilon}_{yy} = \partial u_y(y)/\partial y = -\dot{\epsilon} = -0.05$. What this means is that the actual streaming velocity of the fluid in the contracting dimension for times $t > t_1$ is *not* what these equations assume it should be! In fact, the actual streaming velocity at times $t > t_2$ is shifted by $\approx +0.51$. This contradicts the requirements that the streaming velocity should be stable at all times. In the time interval $t_1 < t < t_2$ an extra amount of linear momentum is introduced in the contracting direction, destroying the symmetry of the flow. During this time the thermostat interprets this excess linear momentum as heat and tries to cool the system. This then stabilizes the system for times $t > t_2$.

The above results suggest that we examine the total linear momentum of the fluid. In Fig. 4(a) we plot the total linear momentum in the y direction as a function of time and observe just such an increase between $t_1 < t < t_2$. More revealing, however, is the fact that the total linear momentum is continually increasing from $t=0$ up to $t \approx t_2$. This is clearly seen in Fig. 4(b), where the scale is magnified. At times $t > t_2$ the fluid appears to have settled into a final non-equilibrium steady state, and the linear momentum remains a constant of the motion. In Fig. 4(c) we plot the total linear momentum of the fluid in the x direction, and observe that, after an initial transient response, it settles to its expected value of zero.

To check the role of the thermostat in the nonconservation of linear momentum, we performed a simulation at a very weak elongation rate ($\dot{\epsilon} = 8.02 \times 10^{-5}$) without a thermostat acting on the fluid. For an unthermostatted fluid the temperature increases as time progresses. If the field is too large the fluid will heat up too rapidly and the simulation will become unstable. However, for such a weak elongation rate the fluid did not heat up significantly within the total simulation time of 60 000 time steps. In Fig. 5 we display the x and y components of the total linear momentum as a function of time, and once again observe that it increases in the direction of contraction, but remains at zero in the direction of expansion. This is the same behavior as in the thermostatted fluid, which suggests that the divergence in the linear momentum in the contraction direction is independent of the thermostating mechanism, at least in the weak field regime. We further note that this divergence is well characterized as exponential, the value of the fitted elongation rate ($\dot{\epsilon}_{\text{fitted}} = 8.13 \times 10^{-5}$) being within numerical error of the actual value of $\dot{\epsilon} = 8.02 \times 10^{-5}$.

DISCUSSION

The central question to ask is the following: why does the total linear momentum in the direction of contraction (y) diverge exponentially, whereas the total linear momentum in the expanding direction (x) behaves as it should and fluctu-

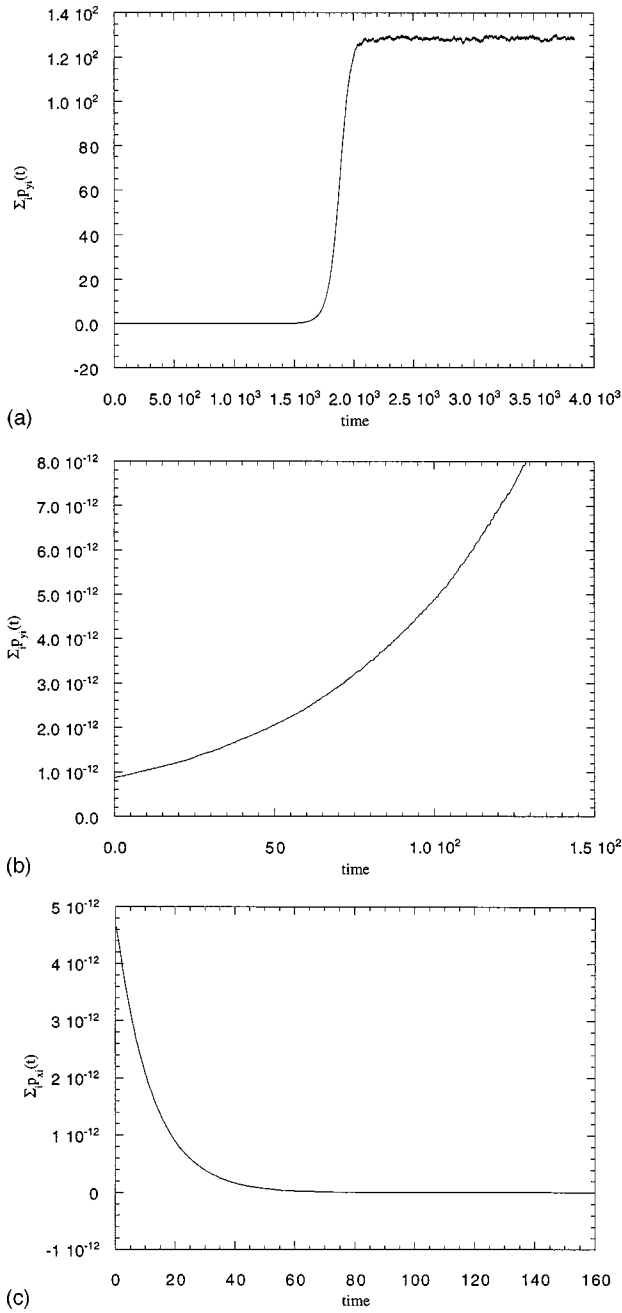


FIG. 4. (a) Total y component of the linear momentum as a function of time. The total peculiar momentum diverges exponentially until $t \approx t_2$. After this time it becomes a constant of the motion and the fluid structure is stabilized. (b) The same as in (a), but now only early times are displayed. On this magnified scale it is clear that the total peculiar momentum diverges exponentially from $t=0$. (c) Total x component of the linear momentum as a function of time.

ates around zero? Furthermore, why do we observe no such violation of momentum conservation in standard NEMD simulations of planar Couette flow?

We consider first the case of planar elongation. For an adiabatic system (such as that displayed in the results for Fig. 5 above) the SLLOD equations of motion¹² are

$$\begin{aligned} \dot{\mathbf{r}}_i &= \frac{\mathbf{p}_i}{m} + \mathbf{r}_i \cdot \nabla \mathbf{u} \\ \dot{\mathbf{p}}_i &= \mathbf{F}_i - \mathbf{p}_i \cdot \nabla \mathbf{u}. \end{aligned} \quad (5)$$

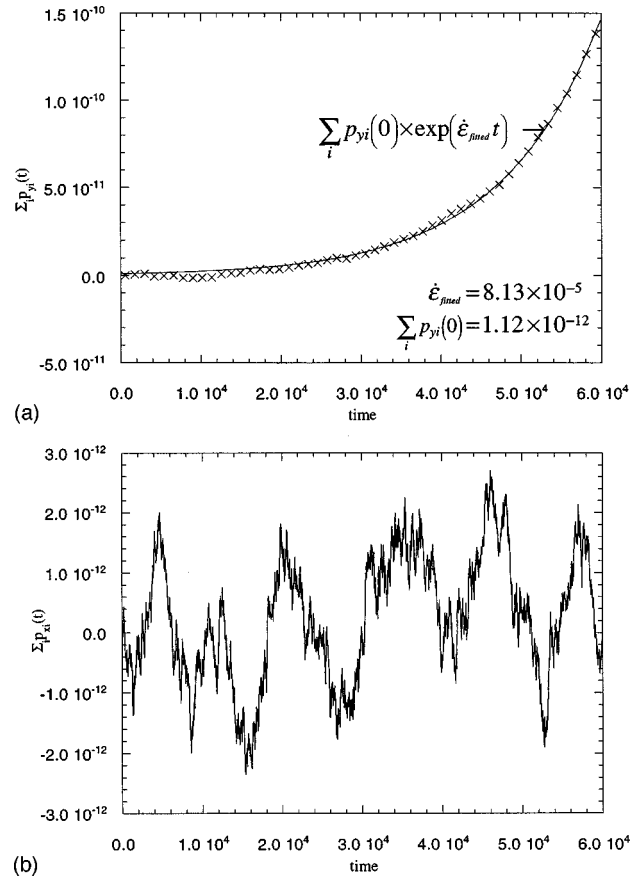


FIG. 5. (a) The total y component of the linear momentum as a function of time for an unthermostatted system with $\dot{\epsilon} = 8.02 \times 10^{-5}$. The plot shows an exponential divergence of the y component of the total linear momentum. Crosses are actual numerical data, while the solid line shows the fit to that data from which a value of $\dot{\epsilon}$ may be estimated. The agreement between the actual and estimated values of $\dot{\epsilon}$ are within 2% of each other. (b) The total x component of the linear momentum as a function of time for the system in (a), which is seen to be time averaged to zero, as expected.

We can write the second equation in terms of x and y components as

$$\dot{p}_{\alpha i} = F_{\alpha i} - \dot{\epsilon}_{\alpha\alpha} p_{\alpha i}, \quad (6)$$

where $\alpha = x$ or y .

Summing over all particles, and observing Newton's third law gives

$$\sum_i \dot{p}_{\alpha i} = -\dot{\epsilon}_{\alpha\alpha} \sum_i p_{\alpha i} \quad (7)$$

or

$$\sum_i dp_{\alpha i} = -\dot{\epsilon}_{\alpha\alpha} \sum_i p_{\alpha i} dt. \quad (8)$$

Defining $P_\alpha = \sum_i p_{\alpha i}$, then $\sum_i dp_{\alpha i} = d(\sum_i p_{\alpha i}) \equiv dP_\alpha$, and Eq. (8) may be written as

$$\frac{dP_\alpha}{P_\alpha} = -\dot{\epsilon}_{\alpha\alpha} dt, \quad (9)$$

which has the simple analytic solution

$$P_\alpha(t) = P_\alpha(0) \exp(-\dot{\epsilon}_{\alpha\alpha} t),$$

i.e.,

$$\sum_i p_{ai}(t) = \sum_i p_{ai}(0) \exp(-\dot{\epsilon}_{\alpha\alpha} t). \quad (10)$$

Noting now that

$$\dot{\epsilon}_{xx} = +\dot{\epsilon},$$

$$\dot{\epsilon}_{yy} = -\dot{\epsilon}, \quad \text{where } \dot{\epsilon} > 0,$$

we obtain the final analytic expressions for the total linear momenta in both the compression and expansion directions, respectively,

$$\begin{aligned} \sum_i p_{yi}(t) &= \sum_i p_{yi}(0) \exp(\dot{\epsilon} t), \\ \sum_i p_{xi}(t) &= \sum_i p_{xi}(0) \exp(-\dot{\epsilon} t). \end{aligned} \quad (11)$$

The implications of Eq. (11) are quite surprising in themselves, in that they state that for a NEMD simulation of PEF, the total linear momentum for a fluid in the contracting (y) direction will *always* tend to diverge exponentially, whereas the total linear momentum of a fluid in the expanding (x) direction will always tend to converge exponentially toward zero. If numerical precision was infinite, then at $t=0$, $\sum_i p_{yi}(0) = 0$ (identically), and hence $\sum_i p_{yi}(t) = 0, \forall t$, and the simulation would conserve momentum and remain stable for all times. As this can never be the case, no matter what the specifics are of the particular numerical integrator chosen, exponential divergence of $\sum_i p_{yi}(t)$ is inevitable. Conservation of momentum is assured in the expanding direction, but can *never* be obtained in the contracting direction under the application of the standard numerical methods.

This result is confirmed by the numerical data in Fig. 5. This type of numerical instability is *not* what is usually associated with kinetic energy conserving integrators,¹⁷ and should be thought of as unique to flows involving contraction of at least one dimension in space. The total linear momentum in this contracting dimension will always be driven to diverge exponentially.

Consider now the case of an adiabatic fluid undergoing planar Couette flow. In this case the appropriate SLLOD equations of motion for the components of peculiar momentum are

$$\begin{aligned} \dot{p}_{xi} &= F_{xi} - \dot{\gamma} p_{yi}, \\ \dot{p}_{yi} &= F_{yi}, \end{aligned} \quad (12)$$

where $\dot{\gamma}$ is the shear strain rate given as $\dot{\gamma} = \partial u_x / \partial y$.

Using Newton's third law for the sum of the forces, we have

$$\sum_i \dot{p}_{xi} = -\dot{\gamma} \sum_i p_{yi} \quad (13a)$$

and

$$\sum_i \dot{p}_{yi} = 0. \quad (13b)$$

Equation (13b) is simply a statement of the conservation of linear momentum in the y direction. Thus, Eq. (13a) becomes

$$\sum_i \dot{p}_{xi} = 0, \quad (14)$$

which itself implies that momentum is conserved in the x direction as well. Thus, any numerical simulation will involve the total linear momentum in both the x and y directions randomly fluctuating about zero. For planar Couette flow the geometry fortuitously demands that the linear momentum is not driven to diverge as it is for planar elongation, or any flow geometry that involves contraction. This is why all simulations of planar Couette flow are numerically stable, even for long simulation times, not considering the usual technical problems associated with numerical drift, which are easily corrected.^{18,19}

Having established the numerical round-off roots of the problem, we now propose two simple and easily implemented solutions, both of which involve only minimal perturbations to the particle trajectories.

The first solution is the most obvious and easily implemented. At each time step simply subtract out the total y momentum from each particle. If $\bar{p}_y \equiv (1/N) \sum_i p_{yi}$, then $p_{yi} \rightarrow p_{yi} - \bar{p}_y$, which guarantees that the sum of the linear momentum in the y direction is always zero at each timestep.

This rezeroing of the total linear momentum involves only very small perturbations to the particle trajectories. Nonetheless, it is an *ad hoc* method and could be criticized because the equations of motion are now no longer fully deterministic and time reversible. However, these two objections can be readily overcome by designing time reversible equations of motion employing a fully deterministic mechanism to constrain the total linear momentum to zero. We demonstrate this by applying Gauss' Principle of Least Constraint¹² to the momentum equation. It is straightforward to show that the new *thermostatted* equations of motion are given as

$$\begin{aligned} \dot{\mathbf{r}}_i &= \frac{\mathbf{p}_i}{m} + \mathbf{r}_i \cdot \nabla \mathbf{u}, \\ \dot{\mathbf{p}}_i &= \mathbf{F}_i - \mathbf{p}_i \cdot \nabla \mathbf{u} - \alpha \mathbf{p}_i - \lambda \mathbf{j}, \end{aligned} \quad (15)$$

where \mathbf{j} is the unit vector in the y direction, and λ is a multiplier determined as

$$\lambda = (1/N) \sum_i [\mathbf{F}_i - \mathbf{p}_i \cdot \nabla \mathbf{u} - \alpha \mathbf{p}_i] \cdot \mathbf{j}. \quad (16)$$

Note that the perturbation applies only to the y component of the momentum. The x component is guaranteed by the dynamics to be conserved, as discussed previously.

As the equations of motion are now thermostatted, we need to evaluate the thermostat multiplier, α . Our preference is to use a Gaussian thermostat,¹² with the appropriate value given as

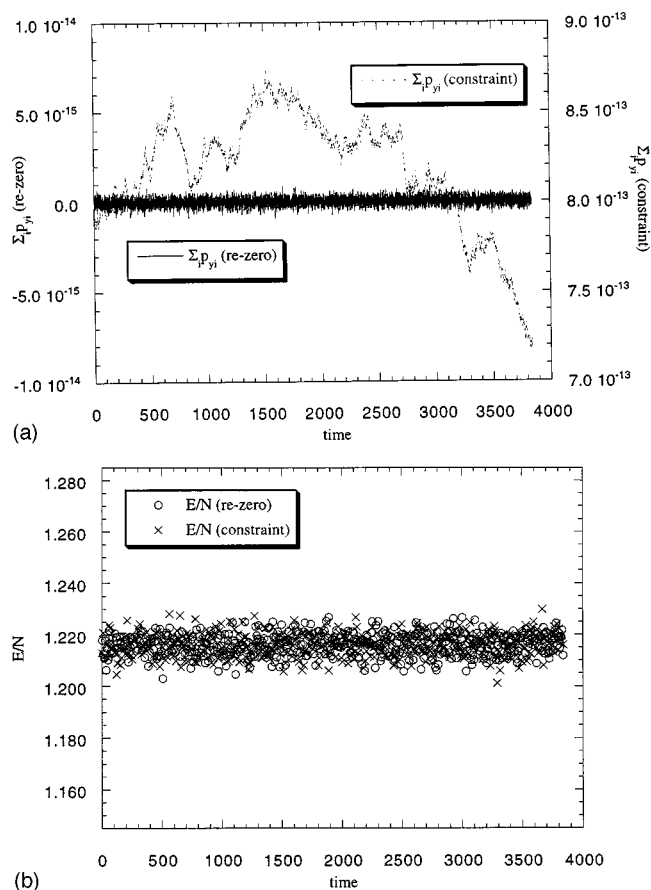


FIG. 6. (a) The total y-component of the linear momentum as a function of time for a thermostatted system ($T=0.722$; $N/V=0.8442$; $\dot{\epsilon}=0.05$) with (i) $\Sigma_i p_{yi}(t)$ set to zero at each time step by *ad hoc* rezeroing, and (ii) with $\Sigma_i p_{yi}(t)$ set to zero by the application of a dynamical Gaussian constraint to the equations of motion. (b) The total internal energy per particle as a function of time for the systems described in (a). The energy for both systems attains a single nonequilibrium steady state, as required, and the fluid no longer experiences a nonequilibrium phase transition.

$$\alpha = \frac{\Sigma_i [\mathbf{p}_i \cdot \mathbf{F}_i - \mathbf{p}_i \cdot (\mathbf{p}_i \cdot \nabla \mathbf{u}) - \lambda \mathbf{p}_i \cdot \mathbf{j}]}{\Sigma_i \mathbf{p}_i^2}. \quad (17)$$

In Fig. 6(a) we display the total linear momentum in the y direction as a function of time for a thermostatted system, using both procedures described above. Both methods are shown to conserve the momentum (i.e., $\Sigma_i p_{yi} = 0$, within statistical errors). The *ad hoc* method does display superior statistics, and because of its simplicity is to be preferred. An equally viable alternative would be to use direct proportional feedback.¹⁸ Finally, in Fig. 6(b) the total internal energy per particle is plotted as a function of time for both methods. There is no measurable statistical difference in the energies (or indeed the pressures) of both systems. Clearly the phase transition has been removed and the fluid structure remains stable throughout the simulation, as confirmed by the equivalence of $\nu(r)$ for both systems (not shown).

CONCLUSION

We have demonstrated that NEMD simulations of planar elongational flow, or indeed any flow in which compression

occurs, are numerically unstable. We have shown that this instability is induced by numerical round-off errors that cause the total linear momentum in the contracting direction to accumulate exponentially in time. This exponential increase reaches a critical value in time, after which the fluid undergoes a catastrophic restructuring that drastically reduces the total internal energy. This lack of momentum conservation is independent of the type of numerical integrator chosen to integrate the equations of motion, and is an unavoidable consequence of the finite precision in the floating point representation of variables inherent in any computer.

We devised two numerical schemes which ensure that momentum is conserved. The first involves *ad hoc* rezeroing of the total momentum in the contracting direction, while the second utilizes a nonholonomic Gaussian constraint. The *ad hoc* method is simpler to use and also displays superior statistics.

We have also shown that NEMD simulations of planar Couette flow do not suffer from this exponential divergence of the total linear momentum. The geometry of the flow fortuitously allows the total momentum to fluctuate around zero.

Finally, we point out that the numerical instability described in this paper was confined to flows in which the elongation rate was relatively weak ($\sim < 0.05$). For higher values of the field we found that the simulations remained stable for long times. Our analysis of the conservation of momentum was based on an unthermostatted fluid, as it was possible to find analytical solutions to the conservation equations, and to compare these solutions with actual numerical results. Naturally, such a fluid had to be under the influence of a very weak field to avoid excessive heating of the fluid (and hence further numerical instability of the system). It was thus not possible to perform unthermostatted simulations for elongation rates above 0.05 for comparison purposes. For thermostatted flows under the influence of weak fields, the thermostat multiplier α is a relatively small term in the momentum equation. Thus, the exponential behavior of the total linear momentum tends to be preserved. However, for larger field strengths the term involving α becomes more dominant, and the corresponding conservation equation is highly nonlinear. This equation cannot be solved analytically, and the numerical results indicate that the exponential dependence of the total linear momentum is destroyed in this higher field region.

ACKNOWLEDGMENT

This work was partially supported by the Cooperative Research Center for Polymers.

- ¹A. M. Kraynik and D. A. Reinelt, Int. J. Multiphase Flow **18**, 1045 (1992).
- ²B. D. Todd and P. J. Daivis, Phys. Rev. Lett. **81**, 1118 (1998).
- ³A. Baranyai and P. T. Cummings, J. Chem. Phys. **110**, 42 (1999).
- ⁴B. D. Todd and P. J. Daivis, Comput. Phys. Commun. **117**, 191 (1999).
- ⁵D. M. Heyes, Chem. Phys. **98**, 15 (1985).
- ⁶M. W. Evans and D. M. Heyes, Mol. Phys. **69**, 241 (1990).
- ⁷M. N. Hounkonnou, C. Pierleoni, and J.-P. Ryckaert, J. Chem. Phys. **97**, 9335 (1992).

- ⁸A. Baranyai and P. T. Cummings, *J. Chem. Phys.* **103**, 10217 (1995).
- ⁹J. D. Weeks, D. Chandler, and H. C. Andersen, *J. Chem. Phys.* **54**, 5237 (1971).
- ¹⁰J. J. Erpenbeck, *Phys. Rev. Lett.* **52**, 1333 (1984).
- ¹¹K. P. Travis, P. J. Daivis, and D. J. Evans, *J. Chem. Phys.* **103**, 1109 (1995).
- ¹²D. J. Evans and G. P. Morriss, *Statistical Mechanics of Nonequilibrium Liquids* (Academic, London, 1990).
- ¹³H. S. Green, *The Molecular Theory of Fluids* (North-Holland-Interscience, New York, 1952).
- ¹⁴J. A. Pryde, *The Liquid State* (Hutchinson University Library, London, 1966).
- ¹⁵W. T. Ashurst and W. G. Hoover, *Phys. Rev. A* **11**, 658 (1975).
- ¹⁶H. J. M. Hanley and D. J. Evans, *Mol. Phys.* **39**, 1039 (1980).
- ¹⁷F. Zhang, D. J. Searles, D. J. Evans, J. S. den Toom Hansen, and D. J. Isbister, *J. Chem. Phys.* **111**, 18 (1999).
- ¹⁸A. Baranyai and D. J. Evans, *Mol. Phys.* **70**, 53 (1990).
- ¹⁹P. J. Daivis, D. J. Evans, and G. P. Morriss, *J. Chem. Phys.* **97**, 616 (1992).